nature chemistry

ARTICLES

PUBLISHED ONLINE: 9 SEPTEMBER 2012 | DOI: 10.1038/NCHEM.1433

Amyloid β-sheet mimics that antagonize protein aggregation and reduce amyloid toxicity

Pin-Nan Cheng[1†], Cong Liu[2†], Minglei Zhao[2], David Eisenberg[2*] and James S. Nowick[1*]

The amyloid protein aggregation associated with diseases such as Alzheimer's, Parkinson's and type II diabetes (among many others) features a bewildering variety of β-sheet-rich structures in transition from native proteins to ordered oligomers and fibres. The variation in the amino-acid sequences of the β-structures presents a challenge to developing a model system of β-sheets for the study of various amyloid aggregates. Here, we introduce a family of robust β-sheet macrocycles that can serve as a platform to display a variety of heptapeptide sequences from different amyloid proteins. We have tailored these amyloid β-sheet mimics (ABSMs) to antagonize the aggregation of various amyloid proteins, thereby reducing the toxicity of amyloid aggregates. We describe the structures and inhibitory properties of ABSMs containing amyloidogenic peptides from the amyloid-β peptide associated with Alzheimer's disease, β_2-microglobulin associated with dialysis-related amyloidosis, α-synuclein associated with Parkinson's disease, islet amyloid polypeptide associated with type II diabetes, human and yeast prion proteins, and Tau, which forms neurofibrillary tangles.

Amyloid aggregation is associated with many intractable protein aggregation diseases, notably including Alzheimer's disease, Huntington's disease, Parkinson's disease, type II diabetes and prion diseases[1–3]. Amyloid fibrils with characteristic highly ordered cross-β structures are the ultimate products of amyloid aggregation. More than 30 proteins have been linked to amyloidogenesis, and they demonstrate enormous variations in relation to their sequences and polymorphic fibril structures[1,4–6]. The fibril formation of a given polypeptide, however, greatly depends on its specific residue order[7,8]. Crystallographic structures of amyloid-like fibrils formed by amyloidogenic peptide fragments suggest that the formation of highly ordered parallel or antiparallel β-sheets and a steric zipper interface between β-sheets are two essential elements for amyloid fibril formation[9,10].

Amyloid fibrils are the most visible evidence of pathology, but soluble oligomers are proving to be more important in amyloid toxicity[11,12]. Although there is an increasing level of evidence showing that these transient, unstable structures are rich in β-sheets, their dynamic and polymorphic properties make amyloid oligomers difficult to study at the atomic level[13–15]. Additional tools are needed to study amyloid oligomers and aggregation and to shed light on controlling these processes.

β-Sheet mimics that can display amyloid β-strands provide a means with which to study amyloid oligomers and aggregation. We previously introduced 42-membered ring macrocyclic β-sheets containing pentapeptide fragments from amyloid-β peptide (Aβ) and tau protein (Tau) to mimic amyloid-like β-sheets and shed light on the structures of transient amyloid oligomers[16,17]. We have also used these macrocyclic β-sheets to inhibit aggregation of the peptide Ac-VQIVYK-NH_2 (AcPHF6), derived from Tau, to provide insights into the aggregation process[18].

The development of a robust chemical model of β-sheets that can tolerate a variety of amino-acid sequences has been challenging, because amyloidogenic sequences vary enormously and because folding of β-sheet mimics largely depends on the amino-acid sequence[1,19]. In this Article, we introduce a new class of β-sheet macrocycles that can tolerate a wide range of amino-acid sequences from amyloid proteins and still fold into β-sheet structures. We call these macrocycles amyloid β-sheet mimics (ABSMs).

ABSM **1** is a 54-membered ring, comprising a heptapeptide β-strand (the upper strand), one Hao unit flanked by two dipeptides (the lower strand) and two δ-linked ornithine ($^{\delta}$Orn) turns (Fig. 1a). The 'upper' β-strand of ABSM **1** incorporates different heptapeptide fragments from Aβ, Tau, yeast Sup35 prion protein (Sup35), human prion protein (hPrP), human β_2-microglobulin (hβ_2M), human α-synuclein (hαSyn) and human islet amyloid

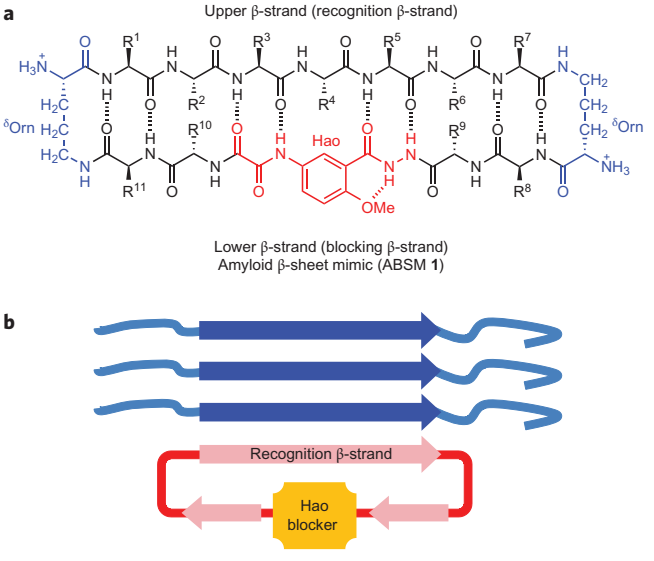

Figure 1 | Design of ABSM 1. a, Representation of ABSM **1** illustrating the upper β-strand (recognition β-strand), the δ-linked ornithine ($^{\delta}$Orn) turn unit and the Hao amino-acid blocker unit. **b**, Representation of ABSM **1** recognizing and blocking amyloid aggregation through β-sheet interactions.

[1]Department of Chemistry, University of California, Irvine, California 92697-2025, USA, [2]UCLA-DOE Institute for Genomics and Proteomics, Howard Hughes Medical Institute, Molecular Biology Institute, University of California, Los Angeles, California, 90095-1570, USA, [†]These authors contributed equally to this work. *e-mail: jsnowick@uci.edu; david@mbi.ucla.edu

polypeptide (hIAPP). Hao is a tripeptide β-strand mimic that not only serves as a template for intramolecular hydrogen bonding, but also minimizes the exposed hydrogen-bonding functionality of the 'lower' strand[20]. This structural design of Hao helps prevent ABSMs **1** from aggregating in solution to form an infinite network of β-sheets; instead, ABSMs **1** dimerize and then further self-assemble into oligomers. The 'upper' and 'lower' strands of ABSM **1** are connected by two $^{\delta}$Orn β-turn mimics[21].

We envisioned that ABSM **1** would fold well because it is conformationally constrained by cyclicity and has a Hao template to promote intramolecular hydrogen bonding and two $^{\delta}$Orn β-turn mimics to promote turn formation. We also envisioned that four pairs of side chains (R^1–R^{11}, R^2–R^{10}, R^6–R^9 and R^7–R^8) would provide stabilizing transannular interactions. We anticipated that the flexibility of the dipeptides flanking Hao in the 'lower' strand would better accommodate the flatness of the Hao template and thus minimize the kinks in the β-strands that we had previously observed in 42-membered ring macrocycles[17].

We designed ABSMs **1** to display exposed heptapeptide β-strands so that these β-strands can recognize and bind their parent amyloid proteins (Fig. 1b). We envisioned recognition between ABSMs **1** and their parent amyloid proteins to take place through the β-sheet interactions observed in amyloid aggregation. Here, we present structural studies of these ABSMs **1** and describe their effect upon amyloid aggregation and toxicity.

Results

Design of ABSMs 1. To test the folding of ABSMs **1**, we selected 16 amyloidogenic heptapeptide β-strands from seven β-sheet-rich amyloid proteins for positions 1–7 in the 'upper' strands (Table 1). ABSMs **1a–g** contain heptapeptide sequences from two important hydrophobic and fibril-forming regions of Aβ associated with Alzheimer's disease, residues 16–23 and 29–40 (refs 5,22). ABSMs **1a–d** and **f** contain native heptapeptide sequences, while ABSMs **1e** and **1g** are G33F and G37F mutants, in which the aromatic residue across from Hao promotes better folding[16]. ABSM **1h** contains residues 7–13 from Sup35, which has been widely used as a model to study amyloid formation[9]. ABSM **1i** contains residues 116–122 from hPrP, which is the infectious agent of prion diseases[23]. ABSM **1j** contains residues 305–311 from Tau, which forms neurofibrillary tangles[24]. ABSM **1k–m** contain residues 62–68 and 63–69 from hβ_2M, which is associated with dialysis-related amyloidosis[25]. ABSMs **1n** and **1o** contain residues 69–75 and 75–81 from hαSyn, which is associated with Parkinson's disease[26]. ABSMs **1p** and **1q** contain residues 11–17 and 26–32 from hIAPP, associated with type II diabetes[27]. We chose polar and hydrophobic residues at positions 8–11 in the 'lower' strands of ABSMs **1** to promote solubility in water and to increase hydrophobic residues that favour β-sheet formation.

Synthesis of ABSMs 1. ABSMs **1** were prepared by synthesizing the corresponding protected linear peptides, followed by solution-phase cyclization and deprotection[28]. The protected linear peptide precursors were synthesized on 2-chlorotrityl chloride resin by conventional Fmoc-based solid-phase peptide synthesis. Macrocyclization was typically performed using HCTU and *N*,*N*-diisopropylethylamine in DMF at a concentration of ~0.5 mM. The ABSMs **1** were isolated in ~20–30% overall yield after high-performance liquid chromatographic purification and lyophilization. Each synthesis produces tens of milligrams of ABSMs **1** as fluffy white solids (for details, see Supplementary Information).

X-ray crystallographic studies of ABSM 1r. X-ray crystallography of ABSM **1r** validated the design of ABSMs **1** (Fig. 2). ABSM **1r** is a homologue of ABSM **1d**, with the Tyr residue in the 'lower' strand replaced with 4-bromophenylalanine for crystallographic phase determination. ABSM **1r** adopts a β-sheet structure in which the

Table 1 | Amino acid sequences and key NOEs of ABSMs 1a–q.

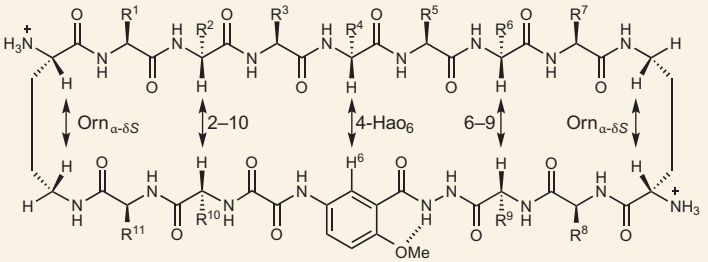

	Sequence	R^1–R^7	R^8–R^{11}	$Orn_{\alpha\text{-}\delta S}$	2–10	$4\text{-}Hao_6$	6–9	$Orn_{\alpha\text{-}\delta S}$	Folding
1a	$A\beta_{16-22}$	KLVFFAE	KLIE	S*	—†	S	S	S	Good
1b	$A\beta_{17-23}$	LVFFAED	KLIE	S	S	S	S	S	Good
1c	$A\beta_{29-35}$	GAIIGLM	KFYK	S	S	S	S	S	Good
1d	$A\beta_{30-36}$	AIIGLMV	KFYK	S	S	S	S	S	Good
1e	$A\beta_{30-36}$ G33F	AIIFLMV	KFYK	S	S	S	S	S	Good
1f	$A\beta_{34-40}$	LMVGGVV	KFYK	S	S	W*	—‡	S	Moderate
1g	$A\beta_{34-40}$ G37F	LMVFGVV	KFYK	S	S	S	S	S	Good
1h	$Sup35_{7-13}$	GQQNNQY	KFYK	W	—‡	—‡	—‡	W	Poor
1i	$hPrP_{116-122}$	AAAGAVV	KFYK	W	W	—‡	—‡	W	Poor
1j	$Tau_{305-311}$	SVQIVYK	EFYK	S	S	S	S	S	Good
1k	$h\beta_2M_{62-68}$	FYLLYYT	KNSA	S	S	S	—†	S	Good
1l	$h\beta_2M_{63-69}$	YLLYYTE	FKVS	W	—‡	—‡	—‡	W	Poor
1m	$h\beta_2M_{63-69}$	YLLYYTE	KVVK	S	—§	S	—§	S	Good
1n	$h\alpha Syn_{69-75}$	AVVTGVT	KFYV	S	S	S	—§	S	Good
1o	$h\alpha Syn_{75-81}$	TAVANKT	VFYK	S	S	S	—§	S	Good
1p	$hIAPP_{11-17}$	RLANFLV	KFYK	S	S	S	S	S	Good
1q	$hIAPP_{26-32}$	ILSSTNV	KFYK	S	S	S	S	S	Good
1r	$A\beta_{30-36}$	AIIGLMV	$KFF^{Br}K$						

*S, strong NOE; W, weak NOE. †NOE not observed due to overlap of proton resonances. ‡NOE not observed. §NOE not observable due to overlap with HOD.

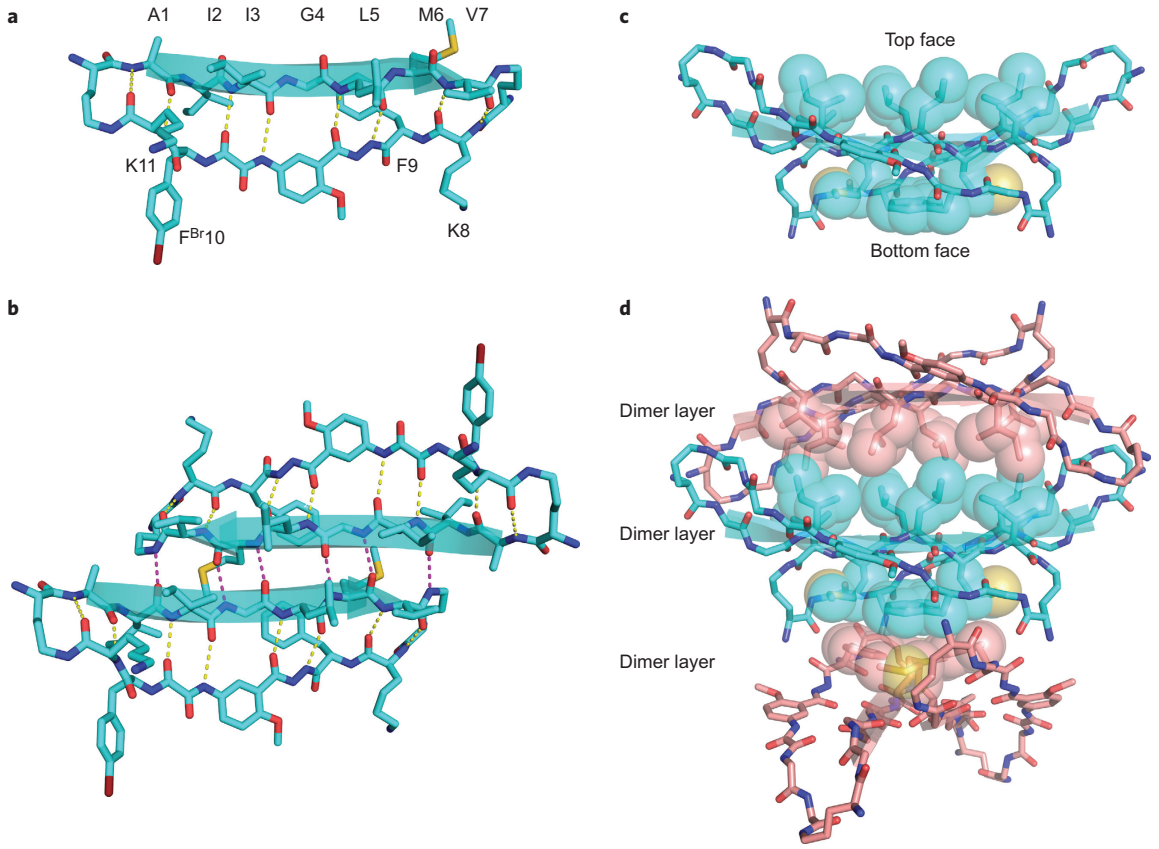

Figure 2 | X-ray crystallographic structure of ABSM 1r, which contains the heptapeptide sequence AIIGLMV ($A\beta_{30-36}$). **a**, The monomer. **b**,**c**, The dimer (top view, **b**; side view, **c**). **d**, Stacked layers of dimer in the crystal lattice. Note that the view in **b** is perpendicular to the β-sheet (top view), whereas the view in **c** and **d** is 90° away, parallel to the β-sheet (side view), and shows the hydrophobic contacts. Some side chains in **c** and **d** have been omitted for clarity.

'upper' and 'lower' strands are intramolecularly hydrogen-bonded to form eight hydrogen bonds (Fig. 2a). The two $^{\delta}$Orn residues of ABSM **1r** fold into β-turn-like conformations, Hao mimics a tripeptide β-strand, and the 'upper' strand displays an exposed heptapeptide β-sheet edge.

ABSM **1r** forms a dimer in the crystal lattice in which the two recognition β-strands come together in an antiparallel β-sheet fashion (Fig. 2b). The β-strands of the dimerization interface are shifted out of register, forming only six hydrogen bonds instead of the eight that would form through in-register contact.

The dimers stack in the crystal lattice, with hydrophobic contacts between the layers of the stack. The Ile, Leu and Val at positions 3, 5 and 7 on the 'top' face of the dimer pack together in one set of hydrophobic contacts 'above' the dimer, while the Met and Phe at positions 6 and 9 on the 'bottom' face of the dimer pack together in another set of hydrophobic contacts 'below' the dimer (Fig. 2c,d). The hydrophobic contacts between the dimer layers appear to be important in the crystallization and supramolecular assembly of ABSM **1r** and may explain the formation of the out-of-register interface within the dimer.

^{1}H NMR studies of ABSMs 1. ^{1}H NMR studies of ABSMs **1a–q** in D_2O solution further validated the design of ABSMs **1** and established that ABSMs **1** generally adopt folded β-sheet structures in solution. The ^{1}H NMR spectra of ABSMs **1** show sharp, disperse resonances at submillimolar and low millimolar concentrations in D_2O solution, suggesting ABSMs **1** to be non-aggregating in water. Antiparallel β-sheets have close contacts between the α-protons of the non-hydrogen-bonded pairs of amino acids, which generally demonstrate strong interstrand nuclear Overhauser effect cross-peaks (NOEs). In ABSMs **1**, these close contacts should involve the α-protons of residues 2 and 10 (2–10) and residues 6 and 9 (6–9). There should also be homologous contacts involving the α-proton of residue 4 and H_6 of Hao (4–Hao_6) and the α- and *pro-S* δ-protons of the $^{\delta}$Orn turns ($Orn_{\alpha-\delta S}$). Table 1 shows these contacts.

All ABSMs, except **1h**, **1i** and **1l**, exhibit most of these key NOEs (Table 1). ABSMs **1a–e**, **1g**, **1j**, **1k** and **1m–q** show strong 2–10, 6–9, 4–Hao_6 and $Orn_{\alpha-\delta S}$ NOEs and thus exhibit good folding. ABSM **1f** shows strong $Orn_{\alpha-\delta S}$ and 2–10 NOEs and a weak 4–Hao_6 NOE, and therefore exhibits moderate folding. ABSMs **1h**, **1i** and **1l** show only $Orn_{\alpha-\delta S}$ NOEs and thus exhibit weak folding. Although the lack of the interstrand NOEs indicates poor folding of ABSMs **1h**, **1i** and **1l**, the $Orn_{\alpha-\delta S}$ NOEs suggest that their $^{\delta}$Orn residues fold at least partially into a β-turn-like conformation. Table 1 summarizes the observed key NOEs and the folding of ABSMs **1**.

Inhibition of amyloid aggregation by ABSMs 1. Thioflavin T (ThT) fluorescence assays and transmission electron microscopy (TEM) studies showed that the ABSMs containing amyloidogenic sequences can inhibit the aggregation of amyloid proteins. We studied the inhibition of $A\beta_{40}$ and $A\beta_{42}$ aggregation by ABSM **1a**, the inhibition of $h\beta_2M$ aggregation by ABSM **1m** and the inhibition of truncated human α-synuclein ($h\alpha Syn_{1-100}$) aggregation by ABSM **1o**.

ThT fluorescence assays show that ABSMs **1a**, **1m** and **1o** effectively delay aggregation of their parent proteins at sub-stoichiometric concentrations in a dose-dependent manner (Fig. 3a–d). At 0.2 equiv., ABSM **1a** delays $A\beta_{40}$ and $A\beta_{42}$ aggregation by 280% and 350%, respectively, and at 0.5 equiv. by 430 and 600% (Fig. 3a,b). Although ThT fluorescence assays show that Aβ aggregation exhibits comparable lag times at 0.5 and 1.0 equiv. of ABSM

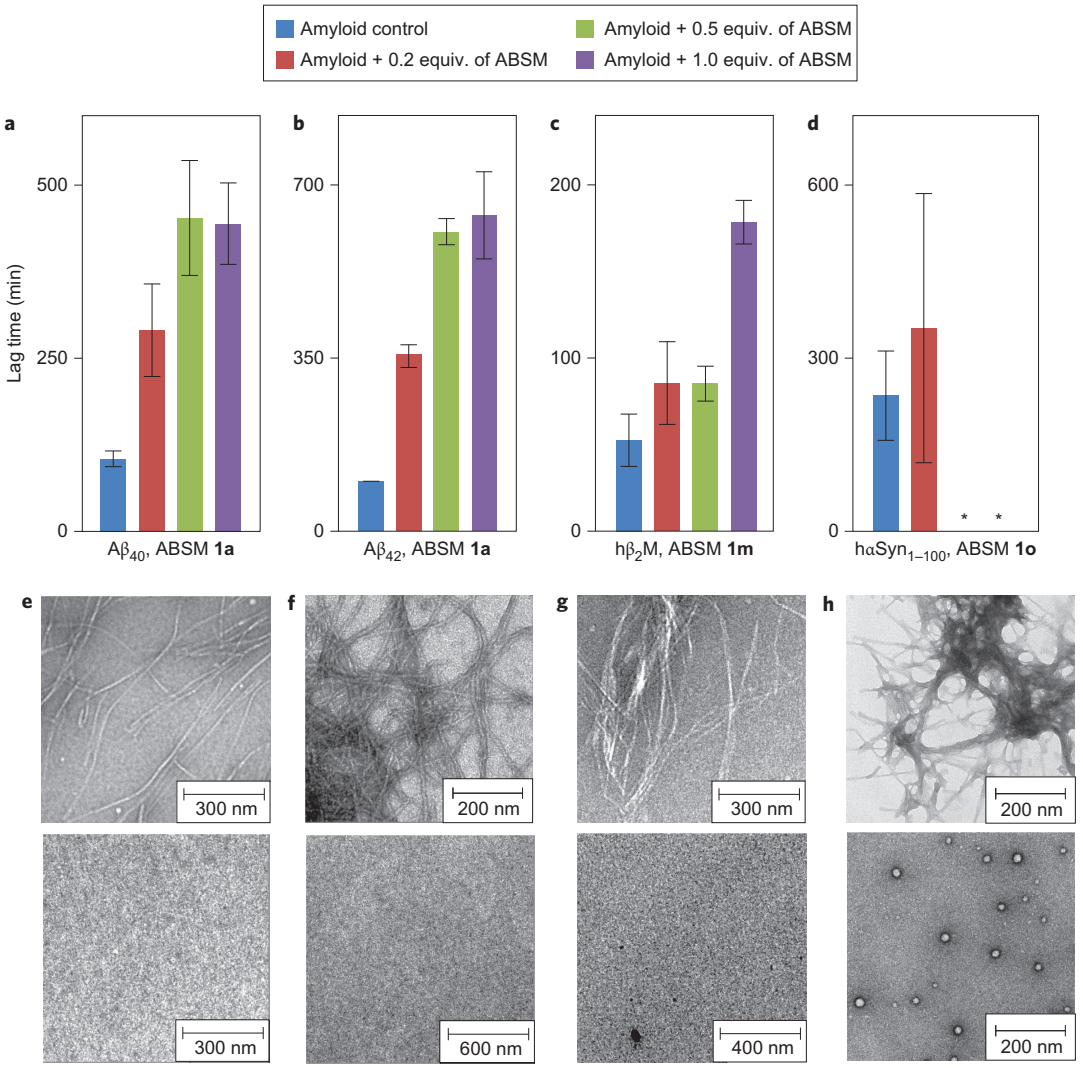

Figure 3 | Effect of ABSMs on inhibition of $A\beta_{40}$, $A\beta_{42}$, $h\beta_2M$ and $h\alpha Syn_{1-100}$ aggregation monitored by thioflavin T fluorescence assays and TEM. **a**, Lag time of $A\beta_{40}$ (20 μM) aggregation in the absence and presence of ABSM **1a**. **b**, Lag time of $A\beta_{42}$ (20 μM) aggregation in the absence and presence of ABSM **1a**. **c**, Lag time of $h\beta_2M$ (30 μM) aggregation in the absence and presence of ABSM **1m**. **d**, Lag time of $h\alpha Syn_{1-100}$ (50 μM) aggregation in the absence and presence of ABSM **1o**. **e**, TEM images of $A\beta_{40}$ (20 μM) after incubation for 6 h without ABSM **1a** (top) and incubation for 6 h with 1.0 equiv. of ABSM **1a** (bottom). **f**, TEM images of $A\beta_{42}$ (20 μM) after incubation for 7 h without ABSM **1a** (top) and incubation for 7 h with 1.0 equiv. of ABSM **1a** (bottom). **g**, TEM of $h\beta_2M$ (30 μM) after incubation for 2 h without ABSM **1m** (top) and incubation for 2 h with 1.0 equiv. of ABSM **1m** (bottom). **h**, TEM of $h\alpha Syn_{1-100}$ (50 μM) after incubation for 72 h without ABSM **1o** (top) and incubation for 72 h with 1.0 equiv. of ABSM **1o** (bottom). Error bars correspond to the standard deviation of four or more sets of experiments. For experimental details, see the Supplementary Information. *$h\alpha Syn_{1-100}$ aggregation exhibits longer lag times with 0.5 and 1.0 equiv. of ABSM **1o** than with 0.2 equiv., with some runs showing complete suppression of aggregation and other runs showing typical sigmoidal curves (for details see Supplementary Fig. S4.)

1a, the growth phases of the aggregation are much slower at 1.0 equiv. than at 0.5 equiv. (for details, see Supplementary Figs S1 and S2). ABSM **1m** delays $h\beta_2M$ aggregation by 160% at 0.2 and 0.5 equiv. and by 340% at 1.0 equiv. (Fig. 3c). ABSM **1o** delays $h\alpha Syn_{1-100}$ aggregation by 150% at 0.2 equiv. (Fig. 3d). Although $h\alpha Syn_{1-100}$ aggregation exhibits longer lag times with 0.5 and 1.0 equiv. of ABSM **1o** than with 0.2 equiv., some runs showed complete suppression of aggregation, and yet other runs showed typical sigmoidal curves. Because of this scatter in the data, precise lag times are not reported (asterisk in Fig. 3d; for details see Supplementary Fig. S4.) TEM studies of samples taken directly from the ThT assays show that Aβ, $h\beta_2M$ and $h\alpha Syn_{1-100}$ form fibrils without ABSMs and do not form fibrils with ABSMs (1.0 equiv.) during the delayed lag time (Fig. 3e–h).

Aβ has been shown to cross-interact with different amyloidogenic proteins containing similar primary sequences[29–31]. To investigate cross-interaction of Aβ with ABSMs, we compared the interaction of Aβ with ABSM **1a** to that with ABSM **1m**, which has a closely homologous sequence, and to that with ABSM **1o**, which does not (Supplementary Fig. S5). ThT fluorescence assays show that ABSM **1m** inhibits Aβ aggregation, like ABSM **1a**, whereas ABSM **1o** has little or no inhibitory effect (Supplementary Fig. S5). This result suggests that structurally homologous ABSMs can not only interact with their parent amyloid proteins but can also cross-interact with different amyloid proteins.

To further investigate the effect of sequence on inhibition, we compared the interaction of ABSM **1a** with $A\beta_{40}$ to that of ABSMs **1b**, **1c**, **1d** and **1f** with $A\beta_{40}$. ThT fluorescence assays show that ABSM **1b** is effective against $A\beta_{40}$ aggregation, whereas ABSMs **1c**, **1d** and **1f** cause little or no inhibition (Supplementary Fig. S6). The inhibition of $A\beta_{40}$ aggregation by both ABSMs **1a** and **1b** indicates that the central hydrophobic sequence $A\beta_{17-21}$ is

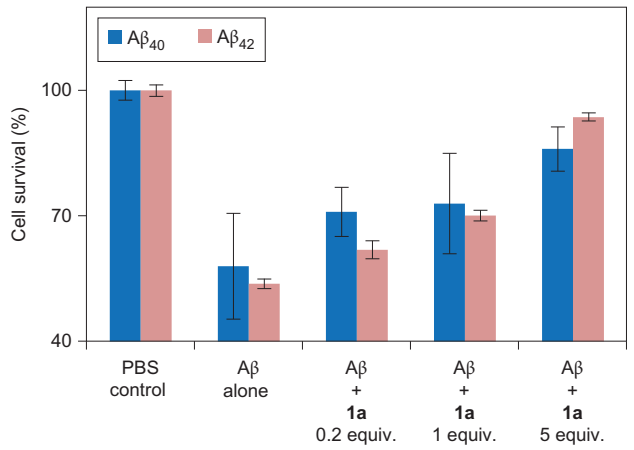

Figure 4 | Effect of ABSM 1a on $A\beta_{40}$ and $A\beta_{42}$ toxicity towards PC-12 cells. Addition of Aβ decreases cell survival when PC-12 cells are cultured for 24 h with preincubated Aβ. Cell survival increases when cells are cultured for 24 h with a preincubated mixture of ABSM **1a** and Aβ in 0.2, 1.0 and 5 molar ratios. Cell survival is given as a percentage relative to controls in which only PBS is added. The cell survival of the PBS controls is taken to be 100%. Error bars correspond to standard deviations of four sets of experiments. For experimental details, see Supplementary Information.

critical to the activity of ABSMs against $A\beta_{40}$ aggregation. This result supports the role of $A\beta_{17-21}$ in Aβ aggregation and suggests that strong interaction of this sequence in these ABSMs with that of the Aβ oligomers delays Aβ aggregation[22,32].

Detoxification of Aβ by ABSM 1a. Cell viability (MTT) assays established that ABSM **1a** reduces the toxicity of $A\beta_{40}$ and $A\beta_{42}$ in PC-12 cells (Fig. 4) and that ABSMs **1a**, **1m** and **1o** exhibit little or no toxicity (Supplementary Fig. S9). We examined the effect of ABSM **1a** on the toxicity of $A\beta_{40}$ and $A\beta_{42}$, because ABSM **1a** exhibits the best inhibitory activity among those studied. We first incubated Aβ monomers (5 μM) without ABSM **1a** to allow Aβ oligomers and fibrils to form. The resulting Aβ mixtures were used directly in cell viability assays. These assays showed that the $A\beta_{40}$ and $A\beta_{42}$ preincubated without ABSM **1a** kill 42% and 46% of the PC-12 cells, respectively, relative to controls in which the cells are incubated in only phosphate-buffered saline (PBS) buffer solutions (Fig. 4).

Cell viability assays further established that preincubation of Aβ with ABSM **1a** rescues the cells in a dose-dependent manner. Preincubation of $A\beta_{40}$ and $A\beta_{42}$ with 0.2 equiv. of ABSM **1a** reduces the death of PC-12 to 29% and 38%, respectively, while pre-incubation with 1.0 equiv. reduces cell death to 27% and 30% and preincubation with 5 equiv. reduces cell death to 14% and 6%. The rescue of these neuron-like cells by ABSM **1a** suggests that ABSMs may reduce the production of toxic amyloid oligomers or bind the oligomers and reduce their toxicity.

Discussion

ABSMs **1** provide a unique tool with which to elucidate the process of amyloid aggregation. Although many of the details of amyloid aggregation remain unclear, nucleation-dependent polymerization, where seeding to form a β-structured nucleus is the rate-determining step, is widely accepted[1,22]. Based on nucleation-dependent polymerization, we propose a model for the potent inhibition of Aβ aggregation by ABSM **1a**. In this model, ABSM **1a** binds early β-structured oligomers and blocks Aβ nucleation (Fig. 5a). Without ABSM **1a**, the unstructured monomer forms β-structured oligomers, which, in the rate-determining step, go on to form a β-structured nucleus that ultimately assembles to form cross-β fibrils. The solid line in Fig. 5a illustrates this pathway. ABSM **1a** creates a new aggregation pathway for the early β-structured oligomers. In this pathway, ABSM **1a** binds the β-structured oligomers to form Aβ-oligomer–ABSM–**1a** complexes and blocks the Aβ oligomer-to-nucleus transition. The dashed line in Fig. 5a illustrates this pathway.

It is significant that ABSM **1a** substantially delays the aggregation of Aβ at sub-stoichiometric concentrations (as low as 1 μM), for example, 0.05 equiv. of ABSM **1a** per equivalent of Aβ (Supplementary Fig. S2), while simple linear peptide fragments derived from Aβ generally show substantial inhibitory effects at stoichiometric or greater concentrations[33,34]. This observation suggests that ABSM **1a** binds a larger oligomer, not the monomer

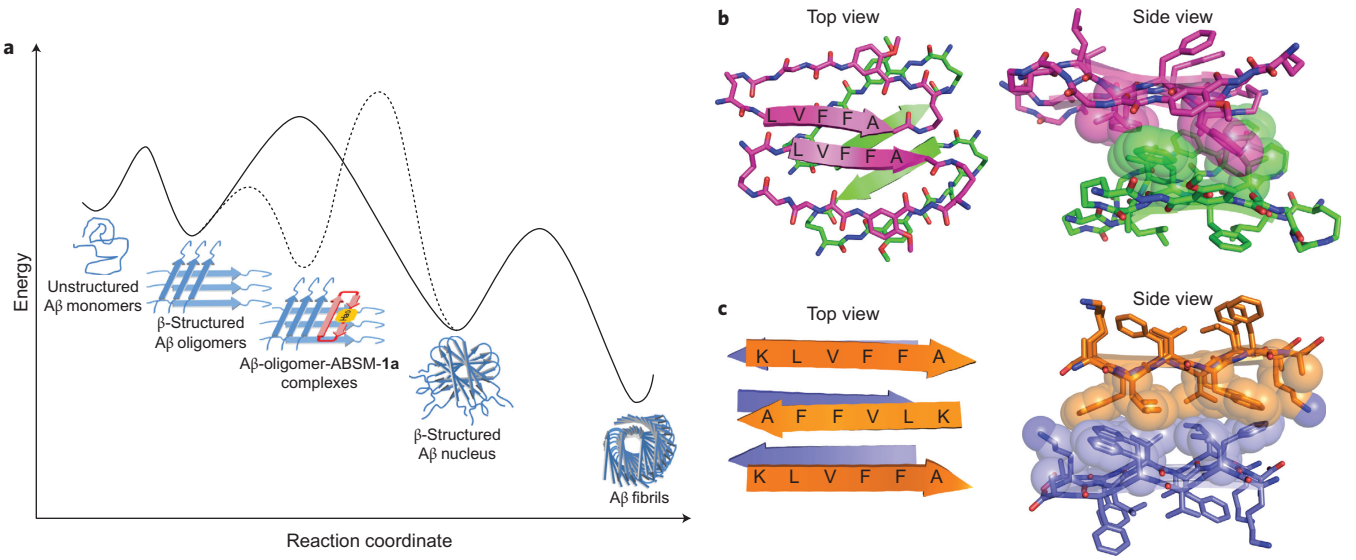

Figure 5 | β-Sheet interactions of Aβ peptides and ABSM 1a. a, Proposed model of inhibition of Aβ aggregation by ABSM **1a**. The solid curve corresponds to a pathway in which Aβ aggregates without ABSM **1a**. The dashed curve corresponds to an alternative pathway in which ABSM **1a** inhibits Aβ aggregation by binding Aβ oligomers. **b**, Crystal structure of a macrocyclic peptide containing pentapeptide sequence LVFFA[17] (PDB ID: 3Q9H). The magenta and green structures correspond to parallel and antiparallel β-sheet dimers formed by the macrocyclic peptide. The side view shows hydrophobic contacts formed between the parallel and antiparallel β-sheet dimers. **c**, Crystal structure of the linear peptide KLVFFA[35] (PDB ID: 3OW9). The orange and purple structures correspond to different layers within the crystal structure. The side view shows hydrophobic contacts between the layers.

or a smaller oligomer such as a dimer, trimer or tetramer. ABSM **1a** binds the early β-structured oligomers more strongly than the unstructured monomers bind oligomers, because the recognition β-strand of ABSM **1a** is preorganized. This preorganization therefore promotes the formation of Aβ-oligomer–ABSM–**1a** complexes. The complexation may occur through edge-to-edge interactions between the hydrogen-bonding edge of ABSM **1a** and exposed hydrogen-bonding groups of the Aβ oligomers, and through face-to-face hydrophobic interactions between ABSM **1a** and the hydrophobic surfaces of the Aβ oligomers. These types of interactions should take place between the hydrophobic sequence $Aβ_{17–21}$ of ABSM **1a** and that of the Aβ oligomers, as observed in the amyloid-related oligomers containing the pentapeptide sequence LVFFA shown in Fig. 5b and the amyloid-like fibrils from the hexapeptide KLVFFA shown in Fig. 5c. Similar interactions should also occur in the interactions of other ABSMs with their parent amyloidogenic peptides and proteins. The stabilization of these complexes creates a higher energy barrier to formation of the β-structured nucleus and thus delays or halts fibril formation. Because ABSM **1a** cannot sequester all of the equilibrating Aβ oligomers, the Aβ monomers and oligomers eventually succumb to thermodynamics and form Aβ fibrils.

The X-ray crystallographic structure of ABSM **1r** may provide insights not only into the stabilization of the dimerization and higher-order supramolecular assembly of ABSMs, but also into the stabilization and structure of intermediates formed during amyloid aggregation. The hydrophobic contacts formed by the Ile, Leu and Val at positions 3, 5 and 7 of ABSM **1r** are akin to the steric zipper of amyloid-like fibrils formed by fragments $Aβ_{16–21}$, $Aβ_{30–35}$, $Aβ_{35–40}$ and $Aβ_{37–42}$ (refs 10 and 35). Both the layered crystal structure of ABSM **1r** and the amyloid-like fibrils are stabilized by hydrophobic contacts. These observations suggest that maximization of both hydrophobic contact and hydrogen bonding is key to stabilizing not only amyloid fibrils but also transient amyloid oligomers[36].

Conclusion

The ABSMs **1** described herein provide a single platform with which to display a variety of amyloidogenic heptapeptide β-strands and provide a rational design for inhibitors to control amyloid aggregation. X-ray crystallographic and ^{1}H NMR studies validate that the design of ABSMs **1**—including cyclicity, Hao template, two ^{δ}Orn β-turn mimics and paired side chains—promotes the formation of β-sheets in which the folding is largely independent of the amino-acid sequence.

ABSMs **1** can be tailored to inhibit the aggregation of different amyloid proteins. The inhibition of Aβ, $hβ_2M$ and $hαSyn_{1–100}$ aggregation by ABSMs **1** indicates that ABSMs containing one hydrogen-bonding edge and one blocking edge are an effective design for inhibitors of amyloid aggregation. The ability of ABSMs **1a**, **1m** and **1o** to inhibit amyloid aggregation and to detoxify amyloid aggregates suggests the potential for therapeutic applications in amyloid-related diseases.

Materials and methods

Synthetic $Aβ_{40}$ was purchased from GL Biochem (Shanghai). $Aβ_{42}$, $hβ_2M$ and $hαSyn_{1–100}$ were expressed in *Escherichia coli* (for details, see Supplementary Information). ABSMs **1** were synthesized as described above (for details, see Supplementary Information). ^{1}H NMR, 2D TOCSY and ROESY experiments with ABSMs **1** were performed in D_2O with DSA (4,4-dimethyl-4-silapentane-1-ammonium trifluoroacetate) as an internal standard at 500 MHz and 298 K (for details, see Supplementary Information). Crystallization, data collection and structure determination for the ABSM **1r** are described in the Supplementary Information. ThT fluorescence assays and TEM studies of Aβ, $hβ_2M$ and $hαSyn_{1–100}$ aggregation with ABSMs **1a**, **1m** and **1o** are described in the Supplementary Information. Cell viability assays to establish the toxicity of ABSMs **1a**, **1m** and **1o** towards HeLa, HEK-293 and PC-12 cells are also described in the Supplementary Information.

Received 26 March 2012; accepted 12 July 2012; published online 9 September 2012

References

1. Chiti, F. & Dobson, C. M. Protein misfolding, functional amyloid, and human disease. *Annu. Rev. Biochem.* **75,** 333–366 (2006).
2. Aguzzi, A. & O'Connor, T. Protein aggregation diseases: pathogenicity and therapeutic perspectives. *Nature Rev. Drug. Discov.* **9,** 237–248 (2010).
3. Bartolini, M. & Andrisano, V. Strategies for the inhibition of protein aggregation in human diseases. *ChemBioChem* **11,** 1018–1035 (2010).
4. Greenwald, J. & Riek, R. Biology of amyloid: structure, function, and regulation. *Structure* **18,** 1244–1260 (2010).
5. Tycko, R. Solid-state NMR studies of amyloid fibril structure. *Annu. Rev. Phys. Chem.***62,** 279–299 (2011).
6. Eichner, T. & Radford, S. E. A diversity of assembly mechanisms of a generic amyloid fold. *Mol. Cell* **43,** 8–18 (2011).
7. Lopez de la Paz, M. & Serrano, L. Sequence determinants of amyloid fibril formation. *Proc. Natl Acad. Sci. USA* **101,** 87–92 (2004).
8. Goldschmidt, L., Teng, P. K., Riek, R. & Eisenberg, D. Identifying the amylome, proteins capable of forming amyloid-like fibrils. *Proc. Natl Acad. Sci. USA* **107,** 3487–3492 (2010).
9. Nelson, R. *et al.* Structure of the cross-β spine of amyloid-like fibrils. *Nature* **435,** 773–778 (2005).
10. Sawaya, M. R. *et al.* Atomic structures of amyloid cross-β spines reveal varied steric zippers. *Nature* **447,** 453–457 (2007).
11. Conway, K. A. *et al.* Acceleration of oligomerization, not fibrillization, is a shared property of both α-synuclein mutations linked to early-onset Parkinson's disease: implications for pathogenesis and therapy. *Proc. Natl Acad. Sci. USA* **97,** 571–576 (2000).
12. Lashuel, H. A., Hartley, D., Petre, B. M., Walz, T. & Lansbury, P. T. Neurodegenerative disease: amyloid pores from pathogenic mutations. *Nature* **418,** 291–291 (2002).
13. Chimon, S. *et al.* Evidence of fibril-like β-sheet structures in a neurotoxic amyloid intermediate of Alzheimer's β-amyloid. *Nature Struct. Mol. Biol.* **14,** 1157–1164 (2007).
14. Bernstein, S. L. *et al.* Amyloid-β protein oligomerization and the importance of tetramers and dodecamers in the aetiology of Alzheimer's disease. *Nature Chem.* **1,** 326–331 (2009).
15. Ono, K., Condron, M. M. & Teplow D. B. Structure–neurotoxicity relationships of amyloid β-protein oligomers. *Proc. Natl Acad. Sci. USA* **106,** 14745–14750 (2009).
16. Woods, R. J. *et al.* Cyclic modular β-sheets. *J. Am. Chem. Soc.* **129,** 2548–2558 (2007).
17. Liu, C. *et al.* Characteristics of amyloid-related oligomers revealed by crystal structures of macrocyclic β-sheet mimics. *J. Am. Chem. Soc.* **133,** 6736–6744 (2011).
18. Zheng, J. *et al.* Macrocyclic β-sheet peptides that inhibit the aggregation of a tau-protein-derived hexapeptide. *J. Am. Chem. Soc.* **133,** 3144–3157 (2011).
19. Gellman, S. H. Minimal model systems for β-sheet secondary structure in proteins. *Curr. Opin. Chem. Biol.* **2,** 717–725 (1998).
20. Nowick, J. S. *et al.* An unnatural amino acid that mimics a tripeptide β-strand and forms β-sheetlike hydrogen-bonded dimers. *J. Am. Chem. Soc.* **122,** 7654–7661 (2000).
21. Nowick, J. S. & Brower, J. O. A new turn structure for the formation of β-hairpins in peptides. *J. Am. Chem. Soc.* **125,** 876–877 (2003).
22. Finder, V. H. & Glockshuber, R. Amyloid-β aggregation. *Neurodegen. Dis.* **4,** 13–27 (2007).
23. Walsh, P., Simonetti, K. & Sharpe, S. Core structure of amyloid fibrils formed by residues 106–126 of the human prion protein. *Structure* **17,** 417–426 (2009).
24. Friedhoff, P., von Bergen, M., Mandelkow, E-M., Davies, P. & Mandelkow, E. A nucleated assembly mechanism of Alzheimer paired helical filaments. *Proc. Natl Acad. Sci. USA* **95,** 15712–15717 (1998).
25. Platt, G. W., Routledge, K. E., Homans, S. W. & Radford, S. E. Fibril growth kinetics reveal a region of $β_2$-microglobulin important for nucleation and elongation of aggregation. *J. Mol. Biol.* **378,** 251–263 (2008).
26. Vilar, M. *et al.* The fold of α-synuclein fibrils. *Proc. Natl Acad. Sci. USA* **105,** 8637–8642 (2008).
27. Luca, S., Yau, W-M., Leapman, R. & Tycko, R. Peptide conformation and supramolecular organization in amylin fibrils: constraints from solid-state NMR. *Biochemistry* **46,** 13505–13522 (2007).
28. Cheng, P-N. & Nowick, J. S. Giant macrolactams based on β-sheet peptides. *J. Org. Chem.* **76,** 3166–3173 (2011).
29. Yan, L-M., Velkova, A., Tatarek-Nossol, M., Andreetto, E. & Kapurniotu, A. IAPP mimic blocks Aβ cytotoxic self-assembly: cross-suppression of amyloid toxicity of Aβ and IAPP suggests a molecular link between Alzheimer's disease and type II diabetes. *Angew. Chem. Int. Ed.* **46,** 1246–1252 (2007).
30. Seeliger, J. *et al.* Cross-amyloid interaction of Aβ and IAPP at lipid membranes. *Angew. Chem. Int. Ed.* **51,** 679–683 (2012).

31. Ma, B. & Nussinov, R. Selective molecular recognition in amyloid growth and transmission and cross-species barriers. *J. Mol. Biol.* **421,** 172–184 (2012).
32. Miller, Y., Ma, B. & Nussinov, R. Polymorphism in Alzheimer Aβ amyloid organization reflects conformational selection in a rugged energy landscape. *Chem. Rev.* **110,** 4820–4838 (2010).
33. Stains, C. I., Mondal, K. & Ghosh, I. Molecules that target beta-amyloid. *ChemMedChem* **2,** 1674–1692 (2007).
34. Sciarretta, K. L., Gordon, D. J. & Meredith, S. C. Peptide-based inhibitors of amyloid assembly. *Methods Enzymol.* **413,** 273–312 (2006).
35. Colletier, J-P. *et al.* Molecular basis for amyloid-β polymorphism. *Proc. Natl Acad. Sci. USA* **108,** 16938–16943 (2011).
36. Laganowsky, A. *et al.* Atomic view of a toxic amyloid small oligomer. *Science* **335,** 1228–1231 (2012).

Acknowledgements

The authors acknowledge support from the NIH (5R01 GM049076, 1R01 GM097562 and 1R01 AG029430), the NSF (CHE-1112188, CHE-0750523 and MCB-0445429) and HHMI. The authors also thank A. Berk and D. Gou for help with tissue culture experiments, and S. Blum for suggestions for Fig. 5a.

Author contributions

P.-N.C., C.L., D.E. and J.S.N. designed the research. P.-N.C., C.L. and M.Z. performed the research. P.-N.C., C.L., M.Z., D.E. and J.S.N. analysed the data. P.-N.C., C.L., M.Z., D.E. and J.S.N. wrote the paper.

Additional information

Supplementary information and chemical compound information are available in the online version of the paper. Reprints and permission information is available online at http://www.nature.com/reprints. Correspondence and requests for materials should be addressed to D.E. and J.S.N.

Competing financial interests

The authors declare no competing financial interests.